

## VU Research Portal

### **A review on substances and processes relevant for optical remote sensing of extremely turbid marine areas, with a focus on the Wadden Sea**

Hommersom, A.; Wernand, M.R.; Peters, S.W.M.; de Boer, J.

***published in***

Helgoland Marine Research  
2010

***DOI (link to publisher)***

[10.1007/s10152-010-0191-6](https://doi.org/10.1007/s10152-010-0191-6)

***document version***

Publisher's PDF, also known as Version of record

[Link to publication in VU Research Portal](#)

***citation for published version (APA)***

Hommersom, A., Wernand, M. R., Peters, S. W. M., & de Boer, J. (2010). A review on substances and processes relevant for optical remote sensing of extremely turbid marine areas, with a focus on the Wadden Sea. *Helgoland Marine Research*, 64, 75-92. <https://doi.org/10.1007/s10152-010-0191-6>

**General rights**

Copyright and moral rights for the publications made accessible in the public portal are retained by the authors and/or other copyright owners and it is a condition of accessing publications that users recognise and abide by the legal requirements associated with these rights.

- Users may download and print one copy of any publication from the public portal for the purpose of private study or research.
- You may not further distribute the material or use it for any profit-making activity or commercial gain
- You may freely distribute the URL identifying the publication in the public portal ?

**Take down policy**

If you believe that this document breaches copyright please contact us providing details, and we will remove access to the work immediately and investigate your claim.

**E-mail address:**

[vuresearchportal.ub@vu.nl](mailto:vuresearchportal.ub@vu.nl)

# A review on substances and processes relevant for optical remote sensing of extremely turbid marine areas, with a focus on the Wadden Sea

Annelies Hommersom · Marcel R. Wernand ·  
Steeff Peters · Jacob de Boer

Received: 16 July 2009 / Revised: 8 January 2010 / Accepted: 15 January 2010 / Published online: 7 February 2010  
© The Author(s) 2010. This article is published with open access at Springerlink.com

**Abstract** The interpretation of optical remote sensing data of estuaries and tidal flat areas is hampered by optical complexity and often extreme turbidity. Extremely high concentrations of suspended matter, chlorophyll and dissolved organic matter, local differences, seasonal and tidal variations and resuspension are important factors influencing the optical properties in such areas. This review gives an overview of the processes in estuaries and tidal flat areas and the implications of these for remote sensing in such areas, using the Wadden Sea as a case study area. Results show that remote sensing research in extremely turbid estuaries and tidal areas is possible. However, this requires sensors with a large ground resolution, algorithms tuned for high concentrations of various substances and the local specific optical properties of these substances, a simultaneous detection of water colour and land–water boundaries, a very short time lag between acquisition of remote sensing and in situ data used for validation and sufficient geophysical and ecological knowledge of the area.

**Keywords** Remote sensing · Tidal flat · Estuary · Turbidity · Suspended particulate matter · Wadden Sea

## Introduction

Monitoring water quality is an important issue in estuaries and tidal flat areas, since they are ecologically and economically important. These environments are very heterogeneous and show extreme concentrations of chlorophyll-a (Chl-a), suspended particulate matter (SPM) or coloured dissolved organic matter (CDOM). Therefore, monitoring with optical remote sensing using generic water quality algorithms is often not possible. Remote sensing of coastal zones is developing on a high speed and although there is literature and in situ data available (e.g. IOCCG 2000; D'Sa and Miller 2003; Brando and Dekker 2003), studies on extremely turbid and heterogeneous areas are still rare and remote sensing research in these areas needs improvements for water quality monitoring (Robinson et al. 2008). The optical properties of estuaries and tidal flat areas are recurrently on the edge of what is described in research on coastal zones, or on the outer ranges of what algorithms are adapted for (e.g. Hellweger et al. 2004).

This review is therefore built up from the opposite direction. It describes the processes taking place in estuaries and tidal areas that lead to the optical heterogeneity and are therefore important for remote sensing, with the perspective to facilitate advances in research and operational remote sensing in these areas, especially in the Wadden Sea (Fig. 1). The examined factors are as follows: extreme concentrations and concentration ranges of SPM, Chl-a, CDOM and turbidity, local, seasonal, and tidal variations and resuspension. With its 450 km length and about 10,000 km<sup>2</sup>, the Wadden Sea is the largest mudflat area in the world, and at the same time the estuary of various rivers (e.g. the river Rhine via Lake IJssel and the North Sea coast, and the rivers Ems, Jade, Weser and Elbe). Because of the extensive research on substances important for

---

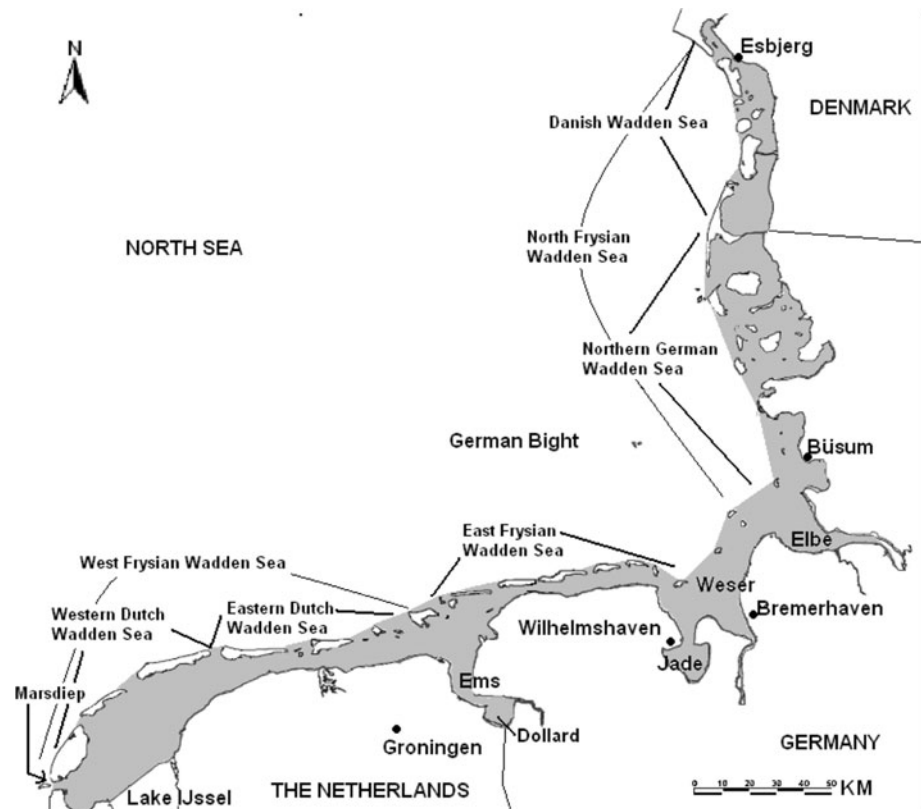
Communicated by H.-D. Franke.

---

A. Hommersom (✉) · S. Peters · J. de Boer  
Institute for Environmental Studies (IVM), VU University,  
De Boelelaan 1087, 1081 HV Amsterdam, The Netherlands  
e-mail: annelies.hommersom@ivm.vu.nl; annelies.hommersom@gmail.com

M. R. Wernand  
Royal Netherlands Institute for Sea Research (NIOZ),  
P. O. Box 59, 1790 AB Den Burg (Texel), The Netherlands

**Fig. 1** The Wadden Sea. For the purpose of this paper, the Wadden Sea is defined as the area between the main land and the barrier islands, indicated in grey



optical remote sensing that has been carried out in this area, it is a perfect location to use as a case study area.

Due to large changes in nutrients and phytoplankton over the last decades (Philippart et al. 2007) in the Wadden Sea, for Chl-*a* only the most recent papers were thought to be relevant for remote sensing purposes now, while older papers about SPM, CDOM and remote sensing were not excluded if they attributed to a better overview. However, remote sensing of ocean colour is a relatively new science (e.g. Spitzer 1981; Spitzer and Folving 1981; Dupouy et al. 1983; IOCCG 2009), which is limiting the time period for this review.

Extreme SPM, CDOM and Chl-*a* concentrations and turbidity, local, seasonal and tidal variations, resuspension plus the influence of these factors on remote sensing data, are examined successively. Already available results of (optical) remote sensing (detecting reflected light in and around the visible spectrum) of water quality in the Wadden Sea are discussed in a separate section. Since these techniques can deliver useful information on for example land–water boundaries, also results from radar (wavelengths <1 mm to 1 m, for example synthetic aperture radar: SAR) and laser (infrared, visible, ultraviolet, for example LIDAR) are examined. Hand-held, air-borne (from a plane) and space-borne (with a satellite) remote sensing research is included. The main focus of this review is on optical remote sensing for water quality monitoring;

therefore, gaps in optical remote sensing and algorithm development in the Wadden Sea are filled with information from other extremely turbid areas. The last section provides recommendations for further development of remote sensing in estuaries and tidal flat areas.

### Extreme concentrations and turbidity

Estuaries and tidal flat areas often show extremely high concentrations of optically active substances (substances having an important influence on the optical properties in the water column). Chl-*a* is elevated due to nutrient input from rivers and land runoff, SPM due to resuspension and CDOM due to river outflow, while the exchanges between estuarine and sea water have a major influence on the fluxes of these substances (Table 1). Concentration ranges found in the Dutch part of the Wadden Sea range for example <1–90 mg m<sup>-3</sup> for Chl-*a* and <1–1,225 g m<sup>-3</sup> for SPM, excluding the extreme values in and near the Dollard where at some occasions SPM was found at concentrations of up to 4,000 g m<sup>-3</sup> (Rijkswaterstaat 2008, including over 20,000 stations between 1976 and 2008). CDOM absorption at 375 nm ranged 0.5–2.5 m<sup>-1</sup> in one measurement campaign (Spitzer 1981; Dupouy et al. 1983). The most extreme SPM concentrations (>1,000 g m<sup>-3</sup>) cited earlier were possibly measured in a not very pronounced layer of “fluid mud”

**Table 1** Known variability of Chl-a, SPM and CDOM over the Wadden Sea

Type of variability	Substance	Minimum	Example value	Maximum	Example value	Unit	Reference
Overall variability	Chl-a	Winter, no wind	1	Spring, in blooms	90	mg m <sup>-3</sup>	Rijkswaterstaat (2008)
	SPM	Summer, deep channel, slack tide, no wind	1	Winter, 1–2 h before slack tide, windy	4,000	g m <sup>-3</sup>	Rijkswaterstaat (2008)
	CDOM	North Sea side, spring or autumn	0.5	Ems river, winter	2.5	Absorption (375) m <sup>-1</sup>	Spitzer (1981) and Dupouy et al. (1983)
Spatial variation	Chl-a	Depends on location blooms, rivers		Depends on location blooms, rivers			–
	SPM	Deep channels	1	Shallows	4,000	g m <sup>-3</sup>	Rijkswaterstaat (2008)
Seasonal variation	CDOM	North Sea side	0.15	Ems river	>2	Absorption (400) m <sup>-1</sup>	Hommersom et al. (2009)
	Chl-a	Winter	Just over 0	Spring	30–70	mg m <sup>-3</sup>	Tillmann et al. (2000)
	SPM	Spring/summer	~40	Winter	~70	g m <sup>-3</sup>	Grossart et al. (2004)
		However: floe formation and high organic matter content in summer		However: less floes and organic matter content in winter			Chang et al. (2006), Grossart et al. (2004)
	CDOM	Spring/summer	~0.03–0.08	Winter	~0.08–0.22	Raman (308 → 420) nm <sup>-1</sup>	Lübben et al. (2009), Laane (1982)
Tidal variation (incl. tidal resuspension)	Chl-a	Depends on blooms, rivers, location, wind		Depends on blooms, rivers, location, wind			
	SPM	Slack tide	5–20	1–2 h before slack tide	14–88	g m <sup>-3</sup>	Poremba et al. (1999)
	CDOM	High tide	0.06 (July) 0.9 (Jan.)	Low tide	0.1 (July) 0.15 (Jan.)	Raman (308 → 420) nm <sup>-1</sup>	Lübben et al. (2009) Values North Sea inlet
Variation in depth (due to resuspension and seepage)	Chl-a	Equal, but with resuspension min. at surface	0–30 (May) 0–15 (July)	Equal, but with resuspension max at bottom	10–100 (May) 0–20 (July)	mg m <sup>-3</sup>	Values Poremba et al. (1999), equal: Lemke et al. (2009)
	SPM	Surface	5–20	Bottom	9–50	g m <sup>-3</sup>	Poremba et al. 1999
	CDOM			Possibly release at the bottom			Lübben et al. (2009)

For each listed type of variability, the columns “Minimum” and “Maximum” represent either the locations or the times at which the minimum and maximum concentrations of Chl-a, SPM and CDOM occur for that type of variability. The example values for one component and one type of variability are taken from publications that list both the minimum and the maximum value. Therefore, the minimum and maximum example values for one type of variability can be compared very well since other causes of variability are mostly constant. The values are considered to be representative for average conditions, and do probably not represent the absolute minima or maxima

(Van Leussen and Van Velzen 1989). Due to the combination of mud with specific properties, flocculation and certain mixing processes, these turbid layers possess the properties of liquids with a buoyancy effect, while the layers keep the mass of suspended sediment (Winterwerp 1999; Wolanski et al. 1988). The resulting fluid mud layers were found at various locations in the world (Winterwerp and Van Kesteren 2004), including the Ems estuary (Van Leussen and Van Velzen 1989), reaching concentrations of several tens to hundreds of kilograms per  $\text{m}^3$  (Winterwerp and Van Kesteren 2004).

The high concentrations of optically active substances lead to a low penetration depth of sunlight. Measures for this penetration depth are the diffuse attenuation coefficient for downwelling light ( $K_d(\lambda)$ ) and the traditional Secchi depth. Because the underwater light field is an important factor for autotrophic organisms (Van Duin et al. 2001) both  $K_d$  and Secchi depth are often reported (De Lange 2000; Marees and Wernand 1990; Cadée and Hegeman 2002; Tillmann et al. 2000).  $K_d$  values for photosynthetically available light are around  $1.4 \text{ m}^{-1}$  in the Marsdiep inlet of the Wadden Sea (De Lange 2000). Secchi depths measured by Rijkswaterstaat (2008) between 1982 and 2008 ranged <0.1 to 4.60 m with a 0.95 percentile of 1.70 for almost 5,000 measurements spread over the Dutch Wadden Sea. The last decade the water became clearer: the 0.95 percentile of the Secchi depths increased to 2.00 m for data collected between 2000 and 2008 (Rijkswaterstaat 2008).

Water quality algorithms should be adapted to these extreme concentrations, concentration ranges and attenuations occurring in estuaries and tidal flat areas. High concentrations of SPM lead to detectable water leaving reflectances and absorption in the near infrared, so that atmospheric correction methods for satellite data based on (near) infrared bands cannot be applied. High SPM concentrations might saturate the spectrum (as shown in the reflectance spectra presented by Lodhi et al. 1997), while the similarity in absorption properties by SPM and CDOM, and to a minor extent by Chl-a (in the blue wavelengths: 400–500 nm), complicates the separation of individual components. A positive side effect of the extremely high concentrations is that, even in these shallow waters, bottom influence is greatly reduced due to the high attenuation of light. Højerslev (2002) concluded that the influence of the bottom on remote sensing reflectance is reduced to negligible levels at 2.2 times the Secchi depth. This would lead to negligible optical influence of the bottom in the Wadden Sea, where the minimum Secchi depths reported were usually reported for stations near or in the (shallow) Dollard, and stations with Secchi depths of 2 m or more were all measured in (deep) channels (Rijkswaterstaat 2008).

## Spatial variation

The dominant spatial structure of the Wadden Sea is formed by tidal channels and flats, fed by North Sea and river water. Deep inlets between the Wadden islands bring in saline North Sea water and accordingly split into several channels and branches, becoming shallower at the more protected places behind the islands where most tidal flats are found. From the main land, the rivers enter the Wadden Sea contributing very distinctive water types. For instance, River Rhine water enters via Lake IJssel which, in spring and summer, contains high concentrations of cyanobacteria (Simis 2006), while the Ems River is very turbid due to high SPM (De Jonge 1992) and (C)DOM (Laane and Kramer 1990) concentrations. The Elbe estuary is relatively clear, as the small organic particles stay in the deepened freshwater part of the estuary (Kerner 2007).

The tidal flats have a high reflection compared to the surrounding water and pixels with complete flat coverage can therefore easily be detected by remote sensing. It is difficult to discriminate pixels at the land–water boundary with partly flat coverage or that are influenced by surrounding flats. Tidal flats, although generally located at the protected places behind the islands, constantly change in shape and place, with a speed of several centimetres a day (Niedermeier et al. 2005; Roelse 2002). At high water, without surfacing flats, the water surface between the islands and the mainland has generally a width of a few kilometres but depending on the location this width varies between 2 and 20 km. This means that the spatial resolution of current ocean colour sensors (e.g.  $\sim 1 \text{ km}$  for MODIS,  $\sim 300 \text{ m}$  for MERIS, IOCCG 2009), should be appropriate for water quality monitoring of the Wadden Sea during high water. Surfacing tidal flats can have sizes of tens of metres square, to some kilometres square, so that during low water at many locations only small channels between flats with widths ranging from smaller than one to several tens of metres remain. However, the deep tidal inlets between the islands are still there with low water. These inlets are 1–3 km wide, and, although winding, some kilometres long. Monitoring water quality during low tide with the current ocean sensors is reduced to these deep channels, because the sensors resolution is not sufficient to monitor most of the small channels. Only SPOT (SPOTimage 2009) has a higher resolution, but has limited spectral bands (2 for 10 m resolution, 3 for 20 m.) which hinders water quality monitoring.

The flats vary in their optical properties and Chl-a content, related to the algae living on the flat. A distinction can be made between relatively stable sand flats and easier erodible mudflats. Mudflats with fine particles have larger quantities of benthic organisms and Chl-a content ( $10\text{--}50 \text{ g m}^{-3}$  in the upper 5 cm) than the sand flats ( $2\text{--}20 \text{ g m}^{-3}$ ).



in the upper 5 cm) (Billerbeck 2005; Colijn and Dijkema 1981), although the sand flats are net autotrophic and have 2–3 times more light availability than the net heterotrophic mudflats (Billerbeck 2005). The crests of the flats generally show larger benthic growth rates and higher stability than troughs, due to excretion products of benthic organisms (Lanuru et al. 2007; De Jonge 1992). This is supposed to be due to the extended emersion times of the crests and, therefore, more effective irradiance (De Jonge 1992; Colijn and Dijkema 1981) or higher temperatures (Rasmussen et al. 1983). At flats emerging for long periods, high salinities and pHs have a negative influence on primary production (Rasmussen et al. 1983). Such flats are stabilised by physical processes such as drying and compaction (Lanuru et al. 2007). Also, the protection of flats from waves is important for their stability and Chl-a content, since storms might destroy the surface layer of benthic organisms. Vice versa, the benthic algae help stabilising the flats section “[Variation due to resuspension](#)”. Colijn and Dijkema (1981) found Chl-a concentrations of  $20 \text{ mg m}^{-2}$  (yearly averages) in the upper 2 cm of sediment at not protected locations, while protected stations had values of  $100 \text{ mg m}^{-2}$ , with extremes  $>200 \text{ mg m}^{-2}$ , again for the upper two centimetres. Due to the growth of benthic organisms, tidal flats add significantly to the primary production and the Chl-a concentration in the Wadden Sea. For example, Cadée and Hegeman (1974) found a production of  $100 \text{ g C m}^{-2} \text{ year}^{-1}$  for the microflora on the tidal flats and only  $20 \text{ g C m}^{-2} \text{ year}^{-1}$  for the water over these flats. Poremba et al. (1999) concluded that high tide results in a supply of primary production from the autotrophic intertidal flats to the heterotrophic channels. Benthic red algae occur in the Wadden Sea in the subtidal zone, but their amount decreased largely the last century (Reise et al. 1989). The species were found to have a distinguishable reflectance spectrum (Kromkamp et al. 2006) and were mapped in an area around the island of Sylt by Reise et al. (1989).

Seagrass and macroalgae attribute to the total Chl-a in the water seen in reflectance spectra, but their spectral shapes are difficult to distinguish (Kromkamp et al. 2006). The sea grass species *Zostera marina* L., or Eelgrass, used to cover large areas of the Wadden Sea; however, it almost completely disappeared in the last century (Bos et al. 2005). The few sea grass fields ( $\sim 60 \text{ km}^2$ ) that left are for 90% located at wave-protected areas in the North Frisian Wadden Sea (Flöser 2004) and consist of *Zostera noltii* (dwarf Eelgrass). Macroalgae typically grow attached to hard substrates, which can in the environment of the Wadden Sea only be found in the form of mussel banks (Dankers and Zuidema 1995), oyster banks, and other (empty) shells. However, they only maintain dense vegetations at sheltered locations (Cadée 1980) since storms remove the macroalgae from more exposed flats. Floating macroalgae can

continue growing, but their contribution to primary production at places other than the sheltered flats with enough substrate is low (Cadée 1980).

In the water column of the Wadden Sea, spatial variation due to the mixing of water from various sources was studied (Brasse et al. 1999; Dick and Schönfeld 1996; Zimmerman and Rommets 1974). Major currents between North Sea, Wadden Sea and rivers partly determine the concentrations of Chl-a and SPM (Grossart et al. 2004), and some researchers could optically distinguish water types and fronts (Hoge and Swift 1982; Reuter et al. 1993).

The spatial distribution of Chl-a over the Wadden Sea is only partly related to the discharges of the rivers. Although Chl-a concentrations and primary production have been subject to much research in the Wadden Sea for a long time (Cadée and Hegeman 2002; De Jonge et al. 1996; Cadée 1986, Postma 1954), the system remains complex and is still not completely understood. Top-down control by predators for example makes the response of phytoplankton to nutrient reduction unpredictable (Philippart et al. 2007). However, it is now known that phytoplankton is mainly light limited (Colijn and Cadée 2003). Evidence for light limitation was found at different stations in the Marsdiep inlet, the Ems-Dollard estuary, and near Norderney and Büsum, Germany (Tillmann et al. 2000; Colijn and Cadée 2003). Only at the end of the spring bloom, in June, a few hours per day nutrients (silicon, phosphorus and in some cases nitrogen) were found to be limiting (Tillmann et al. 2000).

SPM distribution is, due to resuspension, related to water depth (section “[Variation due to resuspension](#)”). Therefore, and because of the accumulation of sediment at sheltered locations, the deeper channels contain generally less suspended matter in most of their water column than the more shallow waters at protected places behind the islands. Local differences in SPM transport occur due to local differences between flow velocities of the ebb and flood current, the dominance of one of the tides or the settling times for particles. Postma (1960) found much higher SPM contributions from the fresh water than in the salt water to the Dollard estuary, while the sediment particles suggested a marine decent and therefore an upstream transport of heavy particles. According to De Jonge (1992), large and small particles are transported upstream in the Ems estuary. However, formation of large size flocs from small particles (Van Leussen 1994) and the turbidity maximum around the upper limit of the brackish water complicate the distribution of small and large particles in this area (Postma 1954, 1960). A net landward transport of all suspended sediment was found in the Danish Wadden Sea (Austen et al. 1999), while in the Dutch Wadden Sea an inward transport of fine particles (silt) was observed (Postma 1954, 1961). Chang et al. (2007) conclude that generally higher ratios of small

to large particles can be found at flats at sheltered locations in the Wadden Sea. However, there is no one-dimensional landward gradient of SPM concentrations or particles sizes, for example, Vinther et al. (2005) found zig-zagging SPM transport in the spit Skallingen, Chang et al. (2007) found lower ratios of small to large particles close to the main land in years with stronger wind conditions than usual.

Starting with the measurements of Spitzer (1981) and Dupouy et al. (1983), studies of the spatial distribution of CDOM have a long history in the Wadden Sea. dissolved organic matter (DOM, which is CDOM plus their uncoloured cousins), dissolved organic carbon (DOC) and yellow substances (another name for CDOM) were found to correlate with freshwater from the rivers (Warnock et al. 1999; Laane and Koole 1982; Laane 1980; Zimmerman and Rommets 1974), leading to a general decrease in CDOM concentration in seaward direction (Lübben et al. 2009). This is a well-known phenomenon. Most DOM in the Ems-Dollard was found to originate from rivers, only a minor part has its origin in phytoplankton production in sea (Laane 1982). However, the situation in the Wadden Sea is complex since it is the estuary of various rivers with different water types. As shown by Laane and Kramer (1990), the rivers Ems, Elbe, Weser and Rhine have different fluorescence rates. CDOM in the Ems (at 440 nm) was found to absorb over  $2 \text{ m}^{-1}$ , while the median absorption over the Wadden Sea area in spring, summer and autumn was  $0.64 \text{ m}^{-1}$  (Table 1) (Hommersom et al. 2009). In the shallow Wadden Sea, pore water adds to the CDOM concentration (Lübben et al. 2009; Boss et al. 2001; Laane and Kramer 1990), while sand beds were found to work as a sink for organic matter that can filter the entire water body of the Wadden Sea within 3–10 days (De Beer et al. 2005). Still, maps of CDOM concentrations over the entire Wadden Sea area as in Hommersom et al. (2009) are sparse.

To conclude, for remote sensing purposes, it is important to be able to distinguish (moving) tidal flats from surrounding water. Using few year-old maps to mask mudflats might not be sufficient due to their migration. Detection of tidal flats will further be discussed in section “Achieved results of remote sensing”. The flats attribute to a high degree to the Chl-a concentrations. Red algae attribute to the reflectance signal but only occur in the Wadden Sea at a few shallow locations (Reise et al. 1989) and are therefore less important for most remote sensing purposes. Sea grass is important at shallow protected locations in the Danish Wadden Sea while macroalgae, with a similar reflectance spectrum, will also only be found at sheltered tidal flats, especially at those with mussel or oyster beds. SPM concentrations are generally larger at shallow location but can follow complex patterns, which are, however, well documented. It is important to recognise that wave-protected locations in the Wadden Sea work as a trap for fine

particles, leading to sediment and SPM compositions that differ from that found in the North Sea. The use of optical remote sensing will add to a better understanding of the processes responsible for the distribution of Chl-a and to the, until this moment, not well-examined CDOM distribution in the Wadden Sea. With high tide and in the deep inlets between the islands, remote sensing of water quality should be possible with the current available optical sensors.

### Seasonal variation

Chl-a concentrations show a large variability over the year. Winter concentrations (average just above  $0 \text{ mg m}^{-3}$ ) are much lower than summer concentrations (between 5 and  $20 \text{ mg m}^{-3}$ ), while in spring (between ~week 10 and 20) a phytoplankton bloom with peak concentrations occurs (Table 1; Tillmann et al. 2000). Although the yearly patterns are similar (Cadée 1980), the overall inter-annual variability is large (Cadée and Hegeman 2002) as well as the maxima measured during spring bloom. For example, Chl-a concentrations during the bloom reported by Tillmann et al. (2000) in 1995 reached just over  $30 \text{ mg m}^{-3}$ , while one year later concentrations were over  $70 \text{ mg m}^{-3}$ . A large contributor to Chl-a abundance in the Wadden Sea is *Pheocystis globosa* (Peperzak 2002). After the spring bloom, the decay of this species leads to the appearance of white reflecting foam at the sea surface, which leads to an increase in the remote sensing reflectance. Anoxia caused by decay of primary producers at the sea bottom (Cadée 1996), is, due to the lower chlorophyll concentrations, nowadays a rare phenomenon in the Wadden Sea. However, it can lead to “black spots” (Michaelis et al. 1992) due to the high concentrations of ferrous sulphide that colour the bottom black at places where anoxia occurs and was in 1996 found to cover surfaces up to  $50 \text{ m}^2$  in the German Wadden Sea (Böttcher et al. 1998). Black spots with such dimensions (1/36th of a MERIS Full Resolution pixel) will influence the measured remote sensing reflectance.

SPM concentrations in autumn and winter were found to be higher (November 1999,  $30\text{--}120 \text{ g m}^{-3}$ , average about  $70 \text{ g m}^{-3}$ ) than in spring and summer (May 2000,  $25\text{--}85 \text{ g m}^{-3}$ , average about  $40 \text{ g m}^{-3}$ ) by Grossart et al. (2004), Lemke et al. (2009) and Andersen and Pejrup (2001). However, Bartholomä et al. (2009) did not find this seasonal pattern. Higher winter concentrations might be mainly due to resuspension by wind induced waves (section “Variation due to resuspension”) that occur more often in winter than in summer. The positive relation between SPM concentrations and higher wind speeds was found by several researchers (e.g. Badewien et al. 2009; Stanev et al. 2009; Bartholomä et al. 2009; Lettmann et al. 2009). However, even when weather conditions were similar, winter

SPM concentrations were higher (Grossart et al. 2004). These generally higher winter SPM concentrations are probably due to the absence of the stabilising effect of benthic organisms that prevents the soil from (tidal) resuspension in summer (section “[Variation due to resuspension](#)”). Organic matter accounts for a higher percentage of the dry weight in spring than in winter (Grossart et al. 2004). This is due to spring phytoplankton blooms and floc formation. Flocs are formed in the calm estuarine waters and account for a large percentage of the total SPM concentration (Van Leussen 1994). Calm weather in combination with high concentrations of organic matter and phytoplankton, and high microbial activity, situations usually occurring in summer, stimulate floc formation (Chang et al. 2006), leading to larger flocs and high settling times of SPM in summer. Floc size increases to current velocities of  $0.1 \text{ m s}^{-1}$  (Chang et al. 2006). Floc sizes are difficult to measure, since flocs easily break down during handling. In the German Wadden Sea maximum sizes around 300–400  $\mu\text{m}$  were found (Bartholomä et al. 2009), while in the Elbe much larger flocs, (with all instruments  $>400 \mu\text{m}$ , with some instruments even  $>1,000 \mu\text{m}$ ) were found (Eisma et al. 1996). At higher (tidal) current velocities floc size decreases with current speed (Bartholomä et al. 2009), large flocs break down, releasing their contents (Chang et al. 2006) to a constant minimum mean size around 250  $\mu\text{m}$  (Bartholomä et al. 2009). Such situations with high currents occur more often in winter so that in winter the concentration and average size of flocs are generally lower. As a result, a net inward transport of organic particles is found in spring and summer, while with the generally higher turbulence in winter a net transport of these particles from the Wadden Sea to the North Sea takes place (Chang et al. 2006; Cadée 1980, section “[Spatial variation](#)”).

CDOM and DOC were found to peak in winter, when the CDOM and DOC flow from rivers and land runoff is high (Lübben et al. 2009; Laane 1982). An increase of DOC in summer, in the outer Ems estuary and the Marsdiep inlet just after the phytoplankton bloom, was supposed to be the result of degradation of phytoplankton (Laane 1982; Cadée 1982). CDOM fluorescence was less influenced by these degradation products, also because the fluorescence of marine CDOM is lower, and showed lower values over the entire spring and summer period (Lübben et al. 2009).

As a result of the higher SPM and CDOM concentrations in winter than in summer, turbidity in the Wadden Sea is higher in winter (Secchi depths between approximately 0.3 and 1.5 m) than in summer (Secchi depths between approximately 0.7 and 2.1 m) (Cadée and Hegeman 2002). Total attenuation values show that in summer the complete Wadden Sea falls within the area where 1% of light penetrates to a maximum of 15 m deep, while in winter 1% light penetrates to a maximum of only to 5 m deep in the complete

Wadden Sea (Visser 1970). However, these patterns can vary in per year (Tillmann et al. 2000).

The seasonal cycles described earlier will be reflected in remote sensing data. For monitoring purposes, it is important to realise that Chl-*a* peak concentrations occur only during a short time and can even be missed with weekly sampling (Cadée 1980), so that cloudy periods may cause problems for monitoring by remote sensing. The formation of flocs is supposed to be a serious difficulty for remote sensing. Flocs have a size and structure that is very different from the SPM particles they consist of, leading to another optical signature of SPM. However, due to the fragility of flocs their optical properties are difficult to measure. General remote sensing algorithms might therefore perform less well in the Wadden Sea or other shallow areas, especially with calm weather, in summer and at slack tide when the largest flocs occur.

### Tidal variation

Tides influence the water depth and therefore determine which tidal flats surface and which are submerged. The variation in tidal level depends on the location: the highest tidal ranges in the Wadden Sea are found in the corner of the German Bight ( $>3 \text{ m}$ ) and the least differences are found near the islands Texel and Fanø ( $\sim 1.5 \text{ m}$ ) (Postma 1982; Dijkema et al. 1980). Storm events alter the water level and thus also the water depth in the tidal area (Stanev et al. 2009; Lettmann et al. 2009). While most South-westerly storms will elevate the water level, strong easterly wind will lower the water level significantly.

Tide causes strong tidal currents in the Wadden Sea, which lead to high mixing. Residence time is typically 11–12 tidal cycles (1 week) (Postma 1982) in the Wadden Sea but much shorter at areas directly connected with the North Sea (Dick and Schönfeld 1996). Therefore, the water column is usually well mixed (Tillmann et al. 2000; Postma 1982). However, salinity differences can cause weak stratification near rivers inputs (Postma 1982). The residence time of the water is not enough to develop autochthonous phytoplankton, which implies that the Wadden Sea species are similar to those found in the North Sea.

Via resuspension, tidal currents have large effects on the SPM concentrations (Poremba et al. 1999; Hommersom et al. 2009). Resuspension will be discussed in more detail in the following section. The formation and break down of flocs shows a tidal pattern (Van der Lee 2000; Eisma and Kalf 1996). Larger flocs are formed in the calm moments of slack tide and, due to a higher collision frequency, at moments with high SPM concentrations around mid-tide. Depending on the location, one of these processes can be dominant (Van der Lee 2000; Eisma and Kalf 1996).



For Chl-a, not always a correlation with tide was found (Poremba et al. 1999; Hommersom et al. 2009). DOM was found to correlate with tides (5% difference between ebb and flood) and salinity, indicating a freshwater source as main contributor (Cadée 1982). Lübben et al. (2009) report tidal fluxes of CDOM in the German Wadden Sea, with maxima when freshwater and pore water mixed with water from the open sea. During periods with significant release of fresh water (February), CDOM fluorescence at a near-shore location during low tide was found to be four times higher than during high tide (Lübben et al. 2009). However, at the station in the tidal inlet, CDOM showed a better correlation with the tidal cycle than at a near-shore station, because at the inland location release of fresh water via flood-gates directly influenced the concentrations (Lübben et al. 2009).

For remote sensing purposes, the tidal influence on depth and surfacing mudflats is important. In the Wadden Sea, the time lag in tidal change is 6 h between far north-east and south-west (Postma 1982). Therefore, one satellite image can contain both locations where tide is high and locations where tide is low. The variations in tidal range and the tidal time lag between areas are important to take into account when a digital elevation model (DEM) is used in combination with satellite data to calculate which tidal flats surface. Tidal variations in Chl-a, SPM and CDOM lead to the necessity to shorten the time difference between remote sensing data acquisition and in situ sampling for calibration.

### Variation due to resuspension

Resuspension is caused by (tidal) currents, wind induced waves, human activity such as dredging (De Jonge 1992), and boating, and by activity of macroinvertebrates such as *Hydrobia ulvae* (Andersen and Pejrup 2002; Austen et al. 1999) or *Arenicola marina* (Cadée 1976). The latter can, for example, rework the upper 6–7 cm sediment of the whole Wadden Sea every year (Cadée 1976). Resuspension is the main contributor to the concentration of SPM (Table 1). However, it also elevates the concentrations of Chl-a, due to resuspension of microphytobenthos (algae attached to particles) and CDOM, due to the release of CDOM from pore water (Lübben et al. 2009). The opposite of resuspension, settling, occurs to SPM and microphytobenthos in calm water, for example during slack tide, and is stimulated by structures that protect areas from currents and waves, such as sea grass. Also macroinvertebrates as mussels and cockles may remove large quantities of Chl-a (Dame et al. 1991; Dame and Dankers 1988) and SPM (Beukema and Cadée 1996; Dankers and Koelemaij 1989; Cadée and Hegeman 1974) from the water column by filter-feeding.

Tides have the largest influence on the occurrence of resuspension (Fig. 2) (Stanev et al. 2009; Poremba et al. 1999). In the Wadden Sea, the time lag between the strongest current and high or low water (slack tide) is 1–2 h (Postma 1982), which is clearly visible in time series where the water level and concentration of SPM is plotted (Fig. 2). In the Dutch Wadden Sea, the flood current has a higher velocity than the ebb current, while at most other places in the Wadden Sea behind the barrier islands the ebb current is stronger (Postma 1982). The ebb current and tidal-induced resuspension are larger with spring tide than with neap tide, while flood currents are not significantly influenced by the moon (Bartholomä et al. 2009). The highest current velocities, up to  $2 \text{ m s}^{-1}$ , occur near the rivers Elbe and Weser. Currents change with the available space: when at low water only small streams are left between the mudflats, all water moves through these small streams causing relatively fast currents (up to  $0.5 \text{ m s}^{-1}$ ). At high tide, when the mudflats are covered with water, the area for water movements is much larger and the currents are less strong (Postma 1982). All these variations in current velocities influence the resuspension rate. Spring tide increases the tidal dynamics that lead to resuspension (Stanev et al. 2009).

If the dynamics in the water column are corrected for tide, wind force was found to be the most important factor for dynamics (Stanev et al. 2009), and therefore for resuspension. At wind speeds of  $2 \text{ m s}^{-1}$  resuspension already takes place (De Jonge 1992). In the Ems estuary, which is relatively protected from the sea, SPM concentrations are mainly influenced by wind generated waves and only to a minor extent by (tidal) currents (De Jonge 1992). SPM concentrations were found to strongly increase after storms (Badewien et al. 2009). Andersen and Pejrup (2001) found SPM concentrations in channels ranging  $<100\text{--}500 \text{ g m}^{-3}$  for a period with little wind in July, while during a storm in December values of  $<100\text{--}almost 1,000 \text{ g m}^{-3}$  were found. (Concentrations measured by Andersen and Pejrup were relatively high because sampling was carried out near the bottom.) Not only wind speed, also the direction of the wind influences the amount of resuspension: onshore winds cause less total resuspension than offshore winds (Badewien et al. 2009; Andersen and Pejrup 2001). Furthermore, the bottom material, benthic diatom content and invertebrates influence the rate of resuspension. In tidal flats with low mud content ( $<20\%$  by weight), mainly sand eroded with an erosion rate six- to tenfold higher than at places with a high mud content, where mud and sand both eroded (Houwing 1999). Benthic diatoms stabilise the mudflat (Lanuru et al. 2007; Austen et al. 1999) with their extracellular polymeric substances (excretion products of algae) (correlation Chl-a content-erosion threshold:  $r = 0.99$ ) (Austen et al. 1999). Wind can damage the film of benthic

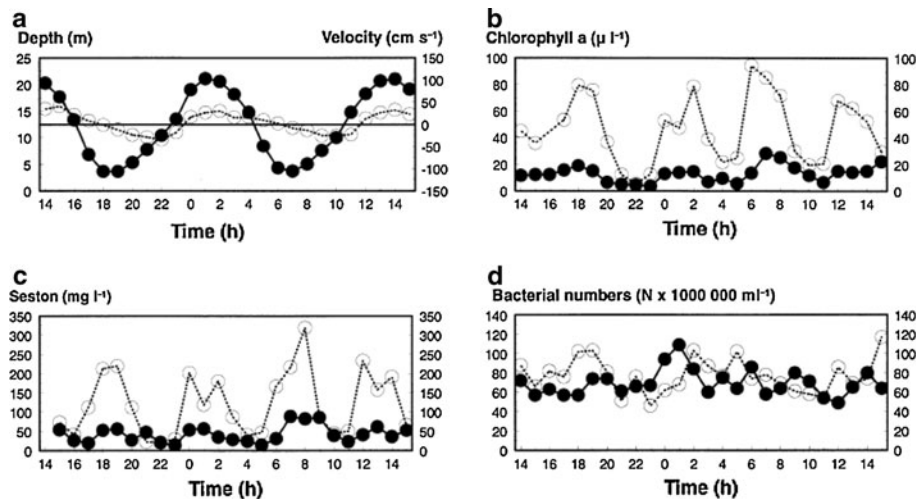


**Fig. 2** Data of May 1994. Variations in **a** water depth (*dotted line*) and current velocity (*solid line*), **b** Chl-*a* ( $\mu\text{g l}^{-1}$ ), **c** Seston or SPM ( $\text{mg l}^{-1}$ ), **d** bacterial cell numbers. For **b**, **c** and **d**, *solid lines* are surface samples, *dotted lines* are bottom samples. This figure was taken with kind permission from Springer Science + Business Media,

Helgoland Marine Research, ‘Tidal impact on planktonic primary and bacterial production in the German Wadden Sea’, 53, 1999, pp. 19–27, K. Poremba, U. Tillmann, K.-J. Hesse, Fig. 2 a, c, e and f. © Springer-Verlag and AWI 1999. Used with kind permission of the authors

diatoms on a tidal flat, making the flat more vulnerable to erosion and causing resuspension of the benthic cells (Colijn and Dijkema 1981; Hommersom et al. 2009). Therefore, also the Chl-*a* concentration increased when the wind speed in the period before sampling had been higher (De Jonge 1992). Deposit feeders were found to destabilise tidal flats (Austen et al. 1999).

Tidal variation in SPM is higher than its seasonal variation (Cadée 1982), but nevertheless, most researchers found resuspension to be more profound in winter than in summer (section “Seasonal variation”). In the results of Grossart et al. (2004), maxima of Chl-*a* and SPM occurred 1 h before slack tide, with higher maxima before high tide than before low tide, which agrees with the moments of maximum tidal currents. The measured Chl-*a* concentrations in May ( $6\text{--}27 \text{ mg m}^{-3}$ ) were mainly due to planktonic species, while in November (concentrations  $3\text{--}10 \text{ mg m}^{-3}$ ) benthic diatoms were dominant, which also points at resuspension. Due to a generally lower current velocity and higher organic matter content, a muddy drape-coverage on the tidal flats can occur in summer, reducing resuspension in summer even more (Chang et al. 2006).

Resuspension leads to higher concentrations of suspended material near the bottom than at the surface. Concentrations and also the variation over a tidal cycle are higher near the bottom, as shown by Poremba et al. (1999). In bottom water, Chl-*a* ranged in one tidal cycle  $10\text{--}100 \text{ mg m}^{-3}$  in May and  $0\text{--}20 \text{ mg m}^{-3}$  in July, while at the surface concentrations ranged  $0\text{--}30 \text{ mg m}^{-3}$  in May and  $0\text{--}15 \text{ mg m}^{-3}$  in July (Poremba et al. 1999). For SPM, the same pattern was seen: near the bottom at a calm station the range over a tidal cycle was  $9\text{--}50 \text{ g m}^{-3}$  and at a station

with high tidal influence  $<22\text{--}220 \text{ g m}^{-3}$ . At the surface, concentrations at a calm station ranged  $5\text{--}20 \text{ g m}^{-3}$  (in July) and at a station with high tidal influence  $14\text{--}88 \text{ g m}^{-3}$  (in May) (Poremba et al. 1999).

Benthic algae (microphytobenthos) account for a substantial part of the primary production in the Wadden Sea (De Jonge 1992; Cadée and Hegeman 1974). Cadée (1980) calculates that the total primary production at deep and shallow locations is similar, because the reduced production due to a short water column at a shallow location is compensated by large production on the tidal flat. In the Ems estuary, 30% of the primary production was due to microphytobenthos in the lower regions, up to 85% in the Dollard (De Jonge 1992). The microphytobenthos on tidal flats accounted for 22%, the resuspended microphytobenthos for 25% and the phytoplankton for 53% of the primary production in the estuary. The resuspended microphytobenthos so accounts for a significant part of the production, and, consequently, the Chl-*a* concentration, in the water column. Generally, microphytobenthos cells are bound to the mud coatings of coarser particles. Cells are present in the same numbers on these aggregates on the intertidal flats as in the channels (De Jonge 1992). Except of these bound microphytobenthos, there are benthic cells living between the sediment particles. These free living cells account generally for a smaller part ( $\sim 30\%$ ) of the benthic primary production (Cadée and Hegeman 1974).

CDOM in pore water is high compared to CDOM in the water column (Lübben et al. 2009; Dupouy et al. 1983; Spitzer 1981). CDOM absorption (375 nm) ranges  $<1\text{--}17 \text{ m}^{-1}$  for pore water, much higher than in the water column (maximum  $\sim 2.5 \text{ m}^{-1}$ ) (Dupouy et al. 1983; Spitzer 1981). Lübben et al. (2009) present profiles of CDOM

fluorescence for these pore waters, with 25 times higher values (2.5 Raman fluorescence units  $^{-nm}$ ) at samples at 5 m deep than at the bottom surface (where values were just over 0 Raman fluorescence units  $^{-nm}$ ). Due to these high concentrations in pore water, release during resuspension of sediment or seepage from sediment (Billerbeck et al. 2006) possibly attributes significantly to the CDOM concentration in the water column (Lübben et al. 2009).

Models of SPM variation in the Wadden Sea including the effect of location, tide and wind (Van Ledden 2003; Stanev et al. 2006, 2007, 2009; Lettmann et al. 2009) can be used to predict SPM patterns, which can be compared with satellite data. Gayer et al. (2006) showed good agreement between their model, in situ data and satellite data in the German Bight, derived with the modelling technique of Pleskachevsky et al. (2005).

For remote sensing purposes, it should be taken in account that the largest concentrations of SPM, and often also Chl-a and CDOM, are found near the bottom, and are therefore in such turbid areas not visible in remote sensing data. The simultaneous resuspension of Chl-a and SPM, and the release of CDOM from sediment is interesting. In oceanic remote sensing, it is common to assume SPM and Chl-a concentrations to be correlated because the SPM consists of algae and algorithms are built on this assumption. In coastal water, these parameters are assumed to be independent because of resuspension of bottom material is independent from phytoplankton blooms. But the oceanic correlation between SPM, Chl-a and CDOM concentrations might partly be true again in very shallow areas like the Wadden Sea due to the simultaneous resuspension of autotrophic organisms with sediment particles. These correlations can be expected at locations that are heavily influenced by tidal currents and during periods with high wind. Resuspension should be visible on satellite data because, due to differences in cell properties (packaging effect) and in pigment content, benthic algae have another spectral shape than pelagic algae. The fast changes due to resuspension with tidal change require almost simultaneous acquisition of remote sensing data and in situ data for validation.

### Achieved results of remote sensing

This section focuses on hand-held, air-borne and space-borne remote sensing research in the Wadden Sea. Already available results of optical remote sensing of the Wadden Sea are discussed. Results obtained with radar and laser on for example land–water boundaries are included. Where optical remote sensing research or algorithm development for water quality monitoring in the Wadden Sea shows large gaps, we refer to literature data from other extremely turbid areas.

### Distinction between land and water

In a tidal flat area, the distinction between land and water is obviously highly relevant. Landsat Thematic Mapper (TM) data (NASA 2009) was used to distinguish tidal flats (64%) and water (36%) (Bartholdy and Folving 1986) and land, water, foreland and clouds (Doerffer and Murphy 1989). Radar and laser have more recently led to good results. Wimmer et al. (2000), Niedermeier et al. (2005) and Wang (1997) detected the land–water line at several moments in the tidal cycle with SAR data and created digital elevation models (DEMs) of it. Wimmer et al. (2000) used air-borne SAR (DEM height accuracies in the order of 5 cm for vegetation-free terrains as the Wadden Sea), while Wang (1997) (DEM height accuracies 5 cm off compared to DEM created with echo sounding) and Niedermeier et al. (2005) (DEM created from SAR data of few years, height accuracies in the order of 30 cm), used space-borne SAR data of the ERS-1 and ERS-2 satellites (ESA 2009). The SAR technique is limited to application in relatively flat terrain without much vegetation. This is typical for tidal flat areas as the Wadden Sea, but it may exclude use in some other estuaries. An advantage of using SAR to create DEMs is that SAR also works with clouds and during night. Brzank and Heipke (2007) and Brzank et al. (2008) presented a method to classify areas as water or mudflat with LIDAR data and to create DEMs of the emerged area. Usually, this classification worked well (90% correct classification), but in case of slowly increasing heights at the water–land boundary the distinction became less precise. This technique can therefore be especially useful in areas where SAR does not work.

Summarising, remote sensing research in the Wadden Sea had led to a proper distinction between land and water. In a flat area where 1.5 m of tidal change causes complete areas to emerge or submerge, even 1 m spatial accuracy is very precise. The challenge now is to combine the knowledge to distinguish land and water with optical remote sensing of water quality.

### Classification of tidal flats

Tidal flats can be classified depending on their characteristics, their coverage and sediment type. Moisture, porosity, organic content and high (>4%) or low silt and clay content could be detected with Landsat TM (Bartholdy and Folving 1986). These data could be classified in mud flats (11%), muddy or mixed flats (20%), wet or moist sand flat (30%), dry sand (25%) and high sand (14%). Doerffer and Murphy (1989) distinguished sea grass and macroalgae on the flats using aerial photography. The tidal flats' sensitivity to erosion was studied with hand-held spectrometers by Hakvoort et al. (1998), who concluded that the Chl-a concentration in

the upper layer of the sediment is the most important factor for increasing stability, with the proportion of fine particles ( $<63\ \mu\text{m}$ ) as the second most important factor. However, the correlation between stability and Chl-a changes depending on the fraction of fine sediment and even disappears in sandy sediments. Twenty years after Bartholdy and Følving (1986), it was possible to map all major properties on tidal flats. Bare sand flats, tidal flats covered with diatoms, green macro-algae, red algae and sea grass (Kromkamp et al. 2006) or flats with the properties of macrophytes, several sediment types and mussel beds could be distinguished (Brockmann and Stelzer 2008) with data from Landsat TM images. SAR data was used for classification of tidal flats sediment types by Gade et al. (2008), who used a technique based on assumptions of sand ripples. Tidal flats in almost the entire Wadden Sea were mapped (Brockmann and Stelzer 2008).

#### Remote sensing of Chl-a

Photosynthetically available radiation has a direct influence on primary production and therefore on Chl-a concentrations. Schiller (2006) derived photosynthetically available radiation in the German Bight with a neural net and a physical model. They used surface reflecting light derived from METEOSAT satellite (EUMETSAT 2009) data and found the neural net to perform best.

The only published Chl-a algorithm based on reflectance spectra measured in the Wadden Sea, mainly the Marsdiep inlet, was constructed by Wernand et al. (2006). This fluorescence algorithm is based on a 2-band difference (670 and 685 nm) and can detect Chl-a between concentrations of 3–300  $\text{mg m}^{-3}$ . In lakes Chl-a concentrations often reach very high values. Therefore, in estuaries algorithms for lakes might be useful. For the extremely turbid Chinese Lake Taihu (Chl-a 4 to  $>400\ \text{mg m}^{-3}$ , SPM  $<10\text{--}280\ \text{g m}^{-3}$  and CDOM 0.27 to  $>2\ \text{m}^{-1}$ ) a three-band ratio algorithm was developed to derive Chl-a concentrations (Zhang et al. 2009), while the Chl-a algorithm of Gons (1999) and Gons et al. (2005), was calibrated for several lakes. This algorithm was later tested in the Belgian coastal zone where high SPM concentrations ( $<10$  to  $>500\ \text{g m}^{-3}$ , Ruddick et al. 2004) occur. It performed for Chl-a concentrations  $>7\ \text{mg m}^{-3}$  better than the standard algorithms of MERIS, MODIS and SeaWiFS (De Cauwer et al. 2004; instrument information: IOCCG 2009), although results were still not satisfactory (Ruddick et al. 2004).

#### Remote sensing of SPM

Satellite SPM detection in the German Bight and Elbe estuary was carried out by Doerffer et al. (1989a, b) and later by Lehner et al. (2004). Doerffer et al. (1989a, b) examined

which parameters could be identified by using Landsat TM data. They found that this sensor was only able to identify the turbidity or SPM, water temperature and atmospheric scattering from seawater. But the SPM could be determined with a high spatial resolution of at least  $120 \times 120\ \text{m}$ . Lehner et al. (2004) used a combination of data from two satellite imaging spectrometers: MOS (IOCCG 2009) for its high spectral resolution (13 bands), and SPOT, which has only 3 bands, for its high spatial resolution (10–20 m). In situ measurements were used to derive a semi-empirical Wadden Sea SPM algorithm and to validate it. SPM calculated with this algorithm from SPOT images was compared to two numerical models for SPM in the Wadden Sea. The authors concluded that the SPOT data can be used to detect errors in SPM models. The error for the SPOT derived data was 40%. Doerffer et al. (2003) were one of the first working on ESA's Medium Resolution Imaging Spectrometer (MERIS) (IOCCG 2009) validation for water constituents. They validated MERIS bottom reflection from atmospheric reflectance for coastal waters (L2) in the German Bight for reflectances measured from a ship. A problem in the atmospheric correction of MERIS was found, resulting in abnormal spectra. Their own atmospheric correction based on a neural network, performed better (Doerffer et al. 2003). Later, this neural net became the standard MERIS algorithm (Doerffer and Schiller 2007). Gemein et al. (2006) used MERIS data to derive SPM in the East Frisian Wadden Sea. Their results were in good comparison with the numerical model of Stanev et al. (2006).

Waves and tidal currents, which are important for resuspension and therefore for SPM (and Chl-a) concentrations, can also be detected by remote sensing. Current velocities were measured with a technique called along-track interferometry (ATI) with an accuracy  $<0.1\ \text{m s}^{-1}$  (Romeisner 2007; Romeisner and Runge 2008). This accuracy is good for locations near the large German rivers (currents up to  $2\ \text{m s}^{-1}$ , Postma 1982) but less useful for intertidal places where currents are much smaller. Horstmann and Koch (2008) used SAR data from ASAR and processed these with an algorithm called WiSAR. They calculated wind directions (bias of  $-1.7^\circ$ ) and wind speeds (bias of  $-1.1\ \text{m s}^{-1}$ ) that showed a good correlation with results from the numerical atmospheric model of the German Weather Service. More precise results were obtained with radar employed from a ship. In a scanned area of about 500 m wide, accuracies were  $0.03\ \text{m s}^{-1}$  which was verified with a vertical Acoustic Doppler Current Profiler (Ziemer 2008). Disadvantage of the technique is the low spatial resolution; an advantage is the opportunity to study local phenomena that can occur in the shallow areas between islands.

Although the MERIS algorithm was partly based on data from the North Sea, the extreme concentrations from the



Wadden Sea were not taken in account. Algorithms to derive SPM at locations with such extreme high SPM concentrations are the one-band algorithm tuned for the Belgian coast (Nechad et al. 2003; Ruddick et al. 2004), the ratio algorithms for the Gironde and Loire estuaries in France (Chl-a  $<5 \mu\text{g l}^{-1}$ , SPM  $<30$  to  $>2,000 \text{ mg l}^{-1}$ , CDOM 0.05–0.26) (Doxaran et al. 2003), and the regression algorithm for the Malaysian coastal waters around Penang (SPM maximum  $>250 \text{ mg l}^{-1}$ ), which takes the specific optical properties of Chl-a and CDOM in account (Lim et al. 2008). Miller and McKee (2004) used Modis Terra (IOCCG 2009) with a ground resolution of  $250 \times 250 \text{ m}$  to develop their SPM ratio algorithm in the complex waters of the northern Gulf of Mexico (US), which is especially useful in narrow water bodies of estuaries or the channels between tidal flats.

### Remote sensing of CDOM

Hoge and Swift (1982) remotely measured CDOM in the German Bight, from a plane. They used a nitrogen-laser transmitter (337 nm) pointed at the sea surface to stimulate in situ fluorescence and were able to detect the fronts of the salt and freshwater masses. Most mixing occurred north-west of the Weser and Elbe rivers over a large area, up to the island of Helgoland. Later, similar research with the newest laser techniques was carried out by Reuter et al. (1993). Chl-a fluorescence (induced with a beam of 500 nm), CDOM fluorescence (induced with a beam of 450 nm) and attenuation (a combination of the two lasers) were measured. Their water type maps, based on CDOM and salinity, showed different patterns in the two investigated seasons (October and May). A linear correlation between salinity and CDOM was found, which makes it theoretically possible to measure salinity by remote sensing (Reuter et al. 1993). Algorithms for CDOM were not developed or validated in the Wadden Sea. An algorithm to derive CDOM in the turbid Conwy estuary (UK) (Chl-a  $<10 \text{ mg m}^{-3}$ , SPM  $<10$  to  $>50 \text{ g m}^{-3}$  and CDOM 0.73 to  $>2 \text{ m}^{-1}$ ) was developed by Bowers et al. (2004). The authors show that the algorithm largely depends on the absorption properties of SPM and propose a three-band algorithm to derive CDOM (and SPM) in other estuaries where the shape of the absorption of CDOM and two ratios of the absorption by particles are known.

### Simultaneous acquisition of various substances and bio-optical modelling

Remote sensing research on various substances in the Wadden Sea water column at the same time dates back to the 1980s. Optical measurements on water quality in the Wadden Sea were done with a spectral irradiance meter by

Spitzer and Wernand (1981), who recognised that particulate matter and dissolved organic matter had a large influence on the measured absorption in the blue part of the spectrum (400–500 nm). Three internal reports of the Netherlands Institute of Sea Research (Spitzer 1981; Spitzer and Folving 1981; Dupouy et al. 1983) describe measurements of upwelling radiance and downwelling irradiance in a shallow area (Balgzand) near the inlet Marsdiep with an Optical Multichannel Analyser (Wernand and Spitzer 1987) from a plane, and an 11-channel radiometer at a measurement tower. At the same time in situ measurements were carried out for Chl-a and pheopigments, SPM and the fluorescence of CDOM (Spitzer 1981). The investigators used a band ratio algorithm and were able to retrieve total and mineral suspended matter, pigment and Chl-a from the measured spectra. From data obtained from a plane also the fluorescence of Chl-a could be detected. Another ratio algorithm (green/blue) was used to determine the brown-green pigment of microphytobenthos (Dupouy et al. 1983). Their conclusion was that remote sensing of the Wadden Sea seemed possible, despite the large SPM concentrations (Dupouy et al. 1983).

Since then, the only attempt to create a model to retrieve concentrations of Chl-a, SPM and CDOM in the Wadden Sea simultaneously was carried out by Peters et al. (2000). They report a complete set of specific inherent optical properties (SIOPs) for Chl-a, SPM and CDOM measured in the Wadden Sea. Bio-optical models use SIOPs to relate concentrations of (usually) SPM, Chl-a and CDOM to reflectance spectra. Inversed bio-optical models can be applied as remote sensing algorithms. Peters et al. (2000) modelled a reflectance spectrum with a bio-optical model according to Gordon et al. (1975). The shapes of their modelled and measured spectrum were similar but the intensity was different. SIOPs can show high variability (Babin et al. 2003a, b), while use of SIOPs that are not suitable for a specific area can lead to large errors (e.g. Astoreca et al. 2006). The data of Peters et al. (2000) were all measured at one location (the Marsdiep inlet) at two days in May 2000. The dataset of Babin et al. (2003a, b) included data from the Wadden Sea, but merged it with data from the North Sea. Due to the short residence time in the Wadden Sea (Postma 1982) phytoplankton species specific phytoplankton absorption and will be similar to that in the coastal North Sea. However, due to the inward transport of fine sediment, the formation of flocs and the CDOM from rivers, the SIOPs of SPM and CDOM are supposed to be different for the Wadden Sea than for the North Sea. Data of Hommersom et al. (2009) are measured over the entire Wadden Sea area, and indeed higher specific SPM absorption values were found than the North Sea. This database lacks the seasonal information on the SIOPs of SPM and Chl-a though. Hence, there is currently not much information on SIOPs to



be the basis for an inverse bio-optical algorithm for the Wadden Sea (Stelzer and Brockmann 2006). An instrument to measure optical properties in the shallow Wadden Sea with a drifter was developed by Puncken et al. (2006). The instrument is called MOSES and floats with the currents at the water surface, measuring fluorescence. Test results show that the technique works for detecting CDOM fluorescence (Puncken et al. 2006). This technique will possibly increase the databases for the Wadden Sea. Another project that will add new information to the longer term optical databases of the Wadden Sea is the measurement pole run by the University of Oldenburg (Reuter et al. 2009).

For the extremely turbid estuaries of the Rhode River (US) and the Huon River (Australia) more optical research on various water column substances was carried out. In the estuary of Rhode River the concentrations of Chl-a are very high ( $\sim 50 \text{ mg m}^{-3}$ , with a spring peak  $>250 \text{ mg m}^{-3}$ ), but SPM ( $<30 \text{ g m}^{-3}$ ) and CDOM ( $<2 \text{ m}^{-1}$ ) are not so extreme (Gallegos et al. 2005), while in the Huon estuary CDOM, with absorption values at 440 nm up to  $14 \text{ m}^{-1}$ , is the extreme property (Clementson et al. 2004). SIOPs and reflectance spectra were studied in the turbid estuaries of the rivers Gironde (France), Loire (France) and Tamar (UK) (Doxaran et al. 2005, 2006) and in the turbid tidal flat area of the Belgian coast (Astoreca et al. 2006). The extreme SPM concentrations of the Gironde, Loire and Belgian coast were mentioned in section “Remote sensing of SPM”; the Tamar River has concentrations similar to those in the Wadden Sea: Chl-a  $<1\text{--}48 \text{ mg m}^{-3}$ , SPM  $2\text{--}800 \text{ g m}^{-3}$  and CDOM 0.04 to  $>3 \text{ m}^{-1}$  (Doxaran et al. 2006). For the Tamar, ratio algorithms were presented to simultaneously derive SPM, CDOM and Chl-a (Doxaran et al. 2005, 2006). The SIOPs from the Tamar River and the Belgian coast can be used for bio-optical modelling, although the SIOPs of these estuaries show large variation between the estuaries. Therefore, SIOPs cannot be used for modelling in other estuaries without validation. About the even more extreme Lake Taihu (China) mentioned earlier (section “Remote sensing of Chl-a”) also much optical information was collected, which was used for optical modelling (Zhang et al. 2009).

Lately, two neural nets, especially for lakes and (extreme) coastal waters were trained. These algorithms, the Case-2 regional (C2R) processor and a lake processor (Doerffer and Schiller 2006a, b) derive Chl-a, SPM and CDOM from satellite data and are available in the “Basis ERS & ENVISAT (A)ATSR and MERIS” Toolbox (BEAM) software. C2R was trained with maximum concentrations of  $112 \text{ mg m}^{-3}$  for Chl-a-a,  $\sim 50 \text{ g m}^{-3}$  for SPM and  $5.0 \text{ m}^{-1}$  for aCDOM at 442 nm (Doerffer and Schiller 2006a, b). The lake processor consists of a boreal and a eutrophic lake processor. Since the eutrophic lake processor

was trained for SPM concentrations similar to that of C2R, a Chl-a range of 0 to  $\sim 30 \text{ mg m}^{-3}$  and the CDOM component split in a humic and a fulvic acid component for which both separately the training range was  $0\text{--}3 \text{ m}^{-1}$  (Doerffer and Schiller 2006a, b), it is also interesting for turbid waters. Another newly developed plug-in for BEAM is meant to reduce the adjacency effect, the effect of highly reflecting vegetation or land on nearby water pixels, and is called ICOL (“improve contrast between ocean and land”) (Santer and Zagolski 2009). The lake processors and ICOL processor were validated with in situ data from lakes (Koponen et al. 2008). No validation was carried out yet in estuarine waters. Although C2R processor was partly trained with German Bight waters, just outside the Wadden Sea, no extensive validation results from this area or elsewhere were found.

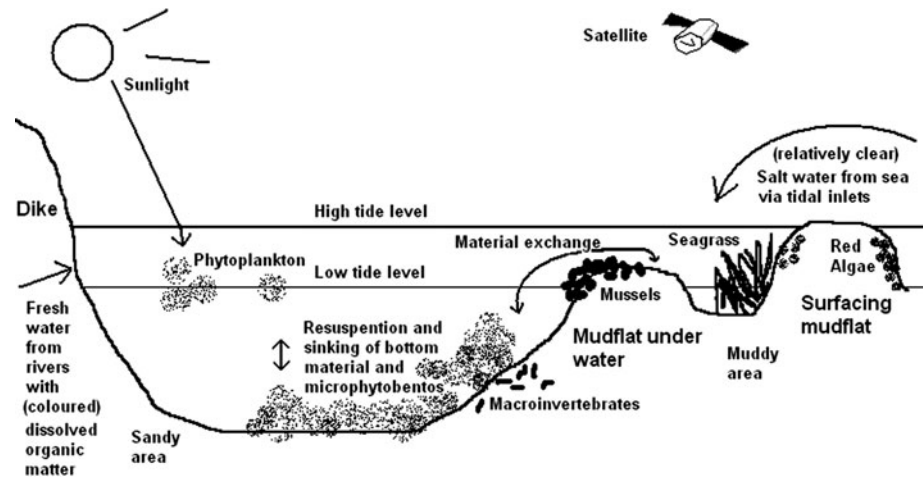
## Conclusions and recommendations

A schematic overview of the substances and processes interesting for optical remote sensing in an estuary—tidal flat area as the Wadden Sea is given in Fig. 3. Spatial variation, such as the inflow of river water, calm areas where fine particles are trapped and flocs are formed, versus deep channels dominated by North Sea water and strong currents, and for example the typical locations of sea grass and macroalgae, are important for the optical heterogeneity in the area (section “Spatial variation”). Seasonal variation is mainly found in the phytoplankton blooms and the formation of flocs of suspended matter (section “Seasonal variation”), while tidal currents (section “Tidal variation”) regulate the salt water inflow from the North Sea and determine which tidal flats emerge and where sand and mud are located. Tidal currents have a large influence on the resuspension (section “Variation due to resuspension”) of SPM and Chl-a (from microphytobenthos) too.

Remote sensing of these extreme heterogeneous and turbid areas is developing. General requirements for coastal remote sensing include, e.g. atmospheric correction adapted to coastal areas (with high concentrations of reflecting substances in the near infrared) (Robinson et al. 2008) and satellites with a high ground resolution. With high water and in the deep inlets between the islands remote sensing of water quality in the Wadden Sea should be possible with the current available optical sensors (section “Spatial variation”). To be able to monitor during low water in the whole area, sensors with the resolution of SPOT (10 m) combined with high spectral resolution should become available.

The extreme turbidity and heterogeneity in tidal flat areas and estuaries puts extra requirements to remote sensing:

**Fig. 3** Schematic overview of substances and processes in the Wadden Sea that influence the colour of the water as detected by optical remote sensing



- Algorithms tuned for the extremely high concentrations of various substances (sections “[Extreme concentrations and turbidity](#)” and “[Achieved results of remote sensing](#)”).
- A simultaneous detection of water colour and land–water boundaries or a model based on a DEM, tidal and weather (wind) information to distinguish land and water (sections “[Spatial variation](#)” and “[Distinction between land and water](#)”)
- Enough local knowledge to interpret the results. Additional information can for example be needed to distinguish locations with macroalgae cover from that with sea grass to understand the distribution of certain sediments or CDOM (section “[Spatial variation](#)”)
- Simultaneous acquisition of remote sensing data and in situ data for validation because of the fast changes as a result of resuspension due to tidal currents (sections “[Tidal variation](#)” and “[Variation due to resuspension](#)”)
- Local knowledge of optical properties to tune the algorithm (section “[Simultaneous acquisition of various substances and bio-optical modelling](#)”). Especially the formation of flocs, with difficult to determine specific absorption properties, might cause problems in optical remote sensing (section “[Seasonal variation](#)”)

Mapping of tidal flats, their coverage and sediment types is developed by various researchers (section “[Classification of tidal flats](#)”), and also the detection of land–water boundaries with a high accuracy is possible (section “[Distinction between land and water](#)”). However, combinations of optical remote sensing algorithms and precise models to distinguish land and water are not known to the authors. A practical way should be found to combine radar measurements with optical measurements, for example by combining data from two ENVISAT instruments: ASAR (SAR) and MERIS (optical).

Waves have a negative influence on the measurements of reflected light (Mobley 1999). To correct for the effect of

waves, simultaneous detection of waves (section “[Remote sensing of SPM](#)”) and optical remote sensing would be very useful.

For the Wadden Sea, but also for many other estuaries and tidal flat areas, knowledge of local inherent optical properties to locally calibrate algorithms is lacking and needs more research (section “[Simultaneous acquisition of various substances and bio-optical modelling](#)”), Robinson et al. 2008). However, existing ratio algorithms developed for areas with extremely high concentrations showed good results (e.g. Chl-a algorithms for the Wadden Sea and Lake Taihu (China), SPM algorithms for the Gironde (France), Loire (France) and Tamar (UK) estuaries and Belgian coast, and CDOM algorithms for the Conwy (UK) and Tamar estuaries (sections “[Remote sensing of Chl-a](#)”, “[Remote sensing of SPM](#)”, “[Remote sensing of CDOM](#)” and “[Simultaneous acquisition of various substances and bio-optical modelling](#)”). The possibilities of these algorithms should be tested and probably calibrated in other areas. Algorithms should specially be validated in areas with similar concentration ranges as the areas they were developed for, such as for the Wadden Sea, the Belgian coast, the Tamar estuary, and to a minor extent the Conwy estuary. Also the C2R and boreal lake algorithms could, after validation, probably be used in these areas (sections “[Achieved results of remote sensing](#)”). All these algorithms are already tuned for extremely high concentrations. If the other four requirements listed earlier are taken in account, water quality monitoring in the Wadden Sea and other extremely turbid tidal and estuarine areas with optical remote sensing should be possible.

**Acknowledgments** Dr. Cadée is thanked gratefully for proofreading the manuscript. Rijkswaterstaat is acknowledged for making their in situ archive available. Dr. Cadée and Dr. Vermaat are thanked gratefully for making their personal libraries on the Wadden Sea available. Figure 2 was taken with kind permission from Springer Science + Business Media, Helgoland Marine Research, “Tidal impact on planktonic primary and bacterial production in the German Wadden

Sea', 53, 1999, Pages 19–27, K. Poremba, U. Tillmann, K.-J. Hesse, Fig. 2 a, c, e and f. © Springer-Verlag and AWI 1999. Used with kind permission of the authors. This project was financed by NWO/SRON Programme Bureau Space Research.

**Open Access** This article is distributed under the terms of the Creative Commons Attribution Noncommercial License which permits any noncommercial use, distribution, and reproduction in any medium, provided the original author(s) and source are credited.

## References

- Andersen TJ, Pejrup M (2001) Suspended sediment transport on a temperate, microtidal mudflat, the Danish Wadden Sea. *Mar Geol* 173:69–85
- Andersen TJ, Pejrup M (2002) Biological mediation of the settling velocity of bed material eroded from an intertidal mudflat, the Danish Wadden Sea. *Estuar Coast Shelf S* 54:737–745
- Astoreca R, Ruddick KG, Rousseau V, Van Mol B, Parent J-Y, Lancelot C (2006) Variability of the inherent and apparent optical properties in a highly turbid coastal area: Impact on the calibration of remote sensing algorithms. *EARSeL e-Proc* 5:1–17
- Austen I, Andersen TJ, Edolvang K (1999) The influence of benthic diatoms and invertebrates on the erodibility of an intertidal mudflat, the Danish Wadden Sea. *Estuar Coast Shelf S* 49:99–111
- Babin M, Morel A, Fournier-Sicre V, Fell F, Stramski D (2003a) Light scattering properties of marine particles in coastal and open ocean waters as related to the particle mass concentration. *Limnol Oceanogr* 48:843–859
- Babin M, Stramski D, Ferrari GM, Claustre H, Bricaud A, Obolensky G, Hoepffner N (2003b) Variations in the light absorption coefficients of phytoplankton, nonalgal particles, and dissolved organic matter in coastal waters around Europe. *J Geophys Res* 108:1–20
- Badewien TH, Zimmer E, Bartholomä A, Reuter R (2009) Towards continuous long-term measurements of suspended particulate matter (SPM) in turbid coastal waters. *Ocean Dynam* 59:227–238
- Bartholdy J, Folving S (1986) Sediment classification and surface type mapping in the Danish Wadden Sea by remote sensing. *Neth J Sea Res* 20:337–345
- Bartholomä A, Kubicki A, Badewien TH, Flemming BW (2009) Suspended sediment transport in the German Wadden Sea—seasonal variations and extreme events. *Ocean Dynam* 59:213–225
- Beukema JJ, Cadée GC (1996) Consequences of the sudden removal of nearly all mussels and cockles from the Dutch Wadden Sea. In: Dworschak PC, Stachowitsch M, Ott JA (eds) Influences of organisms on their environment, the role of episodic events: proceedings of the 29th European marine biology symposium Vienna 1994. *PSZN I: Mar Ecol* 17:279–289
- Billerbeck M (2005) Pore water transport and microbial activity in intertidal Wadden Sea sediments. Dissertation, Bremen University
- Billerbeck M, Werner U, Polerecky L, Walpersdorf E, De Beer D, Huettel M (2006) Surficial and deep pore water circulation governs spatial and temporal scales of nutrient recycling in intertidal sand flat sediment. *Mar Ecol-Progress Series* 326:61–77
- Bos AR, Dankers N, Groeneweg AH, Hermus DCR, Jager Z, De Jong DJ, Smit T, De Vlas J, Van Wieringen M, Van Katwijk MM (2005) Eelgrass (*Zostera marina* L.) in the western Wadden Sea: monitoring, habitat suitability model, transplantations and communication. In: Mees HJ-LJ, Salman A, Seys J, Van Nieuwenhuysen H, Dobbelaere I (eds) Proceedings 'Dunes and Estuaries 2005'—international conference on nature restoration, practices in European coastal habitats. VLIZ Special Publication 19, Belgium, pp 95–109
- Böttcher M, Oelschläger B, Höepner T, Brumsack H-J, Rullkötter J (1998) Sulfate reduction related to the early diagenetic degradation of organic matter and “black spot” formation in tidal sandflats of the German Wadden Sea (southern North Sea): stable isotope ( $^{13}\text{C}$ ,  $^{34}\text{S}$ ,  $^{18}\text{O}$ ) and other geochemical results. *Org Geochem* 29:1517–1530
- Boss E, Pegau WS, Ron J, Zaneveld V, Barnard AH (2001) Spatial and temporal variability of absorption by dissolved material at a continental shelf. *J Geophys Res* 106:9499–9507
- Bowers DG, Evans D, Thomas DN, Ellis K, Williams PJ, Le B (2004) Interpreting the colour of an estuary. *Estuar Coast Shelf S* 59:13–20
- Brando VE, Dekker AG (2003) Satellite hyperspectral remote sensing for estimating estuarine and coastal water quality. *IEEE T Geosci Remote* 41:1378–1387
- Brasse S, Reimer A, Seifert R, Michaelis W (1999) The influence of intertidal mudflats on the dissolved inorganic carbon and total alkalinity distribution in the German Bight, southeastern North Sea. *J Sea Res* 42:93–103
- Brockmann C, Stelzer K (2008) Optical remote sensing of intertidal flats. In: Barale V, Gade M (eds) Remote sensing of the European Seas. Springer, The Netherlands, pp 117–128
- Brzank A, Heipke C (2007) Supervised classification of water regions from lidar data in the Wadden Sea using a fuzzy logic concept. In: Proceedings of the ISPRS workshop on laser scanning and Silvi-Laser, Espoo 2007, Finland. International Archives of Photogrammetry, Remote Sensing, and Spatial Information Sciences 36, Part 3/W52, pp 90–95
- Brzank A, Heipke C, Goepfert J, Soergel U (2008) Aspects of generating precise digital terrain models in the Wadden Sea from lidar-water classification and structure line extraction. *ISPRS J Photogramm* 63:510–528
- Cadée GC (1976) Sediment reworking by *Arenicola marina* on tidal flats in the Dutch Wadden Sea. *Neth J Sea Res* 10(4):440–460
- Cadée GC (1980) Reappraisal of the production, import of organic carbon in the Western Wadden Sea. *Neth J Sea Res* 14:305–322
- Cadée GC (1982) Tidal and seasonal variation in particulate and dissolved organic matter in the western Dutch Wadden Sea and the Marsdiep tidal inlet. *Neth J Sea Res* 15(2):220–249
- Cadée GC (1986) Increased phytoplankton primary production in the Marsdiep area (western Dutch Wadden Sea). *Neth J Sea Res* 20(2–3):285–290
- Cadée GC (1996) Accumulation and sedimentation of *Phaeocystis globosa* Wadden Sea. *J Sea Res* 36:321–327
- Cadée GC, Hegeman J (1974) Primary production of the benthic microflora living on tidal flats in the Dutch Wadden Sea. *Neth J Sea Res* 8(2–3):260–291
- Cadée GC, Hegeman J (2002) Phytoplankton in the Marsdiep at the end of the 20th century; 30 years monitoring biomass, primary production, and *Phaeocystis* blooms. *J Sea Res* 48:97–110
- Chang TS, Joerdel O, Flemming BW, Bartholomä A (2006) The role of particle aggregation/disaggregation in muddy sediment dynamics and seasonal sediment turnover in a back-barrier tidal basin, East Frisian Wadden Sea, southern North Sea. *Mar Geol* 235:49–61
- Chang TS, Flemming BW, Bartholomä A (2007) Distinction between sortable silts and aggregated particles in muddy intertidal sediments of the East Frisian Wadden Sea, southern North Sea. *Sediment Geol* 202:453–463
- Clementson LA, Parslow JS, Turnbull AR, Bonham PI (2004) Properties of light absorption in a highly coloured estuarine system in south-east Australia which is prone to blooms of the toxic dinoflagellate *Gymnodinium catenatum*. *Estuar Coast Shelf S* 60:101–112
- Colijn F, Cadée GC (2003) Is phytoplankton growth in the Wadden Sea light or nitrogen limited? *J Sea Res* 49:83–93

- Colijn F, Dijkema KS (1981) Species composition of benthic diatoms and distribution of chlorophyll *a* on an intertidal flat in the Dutch Wadden Sea. *Mar Ecol-Progress Ser* 4:9–21
- D'Sa ED, Miller RL (2003) Bio-optical properties in waters influenced by the Mississippi River during low flow conditions. *Remote Sens Environ* 84:538–549
- Dame RF, Dankers N (1988) Uptake and release of materials by a Wadden Sea Mussel Bed. *J Exp Mar Biol Ecol* 118:207–216
- Dame RF, Dankers N, Prins T, Jongsma H, Smaal A (1991) The influence of mussel beds on nutrients in the Western Wadden Sea and Eastern Scheldt estuaries. The influence of mussel beds on nutrients in the Western Wadden Sea and Eastern Scheldt estuaries. *Estuaries Coasts* 4:130–138
- Dankers N, Koelemaj K (1989) Variations in the mussel population of the Dutch Wadden Sea in relation to monitoring of other ecological parameters. *Helgoländer Meeresun [Helgoland Mar Res]* 43:529–535
- Dankers N, Zuidema DR (1995) The Role of the Mussel (*Mytilus edulis* L.) and Mussel Culture in the Dutch Wadden Sea. *Estuaries* 18:71–80
- De Beer D, Wenzhöfer F, Ferdelman TG, Boehme SE, Huettel M, Van Beusekom JEE, Böttcher ME, Musat N, Dubilier N (2005) Transport and mineralization rates in North Sea sandy intertidal sediments, Sylt-Rømø Basin, Wadden Sea. *Limnol Oceanogr* 50:113–127
- De Cauwer V, Ruddick K, Park Y.-J, Nechad B, Kyramarios M (2004) Optical remote sensing in support of eutrophication monitoring in the southern North Sea. *EARSeL eProc* 3:208–224
- De Jonge VN (1992) Physical processes and dynamics of microphytobenthos in the Ems estuary (the Netherlands) Dissertation, Groningen University
- De Jonge VN, Bakker JF, Van Stralen M (1996) Recent changes in the contributions of river Rhine and North Sea to the eutrophication of the Western Dutch Wadden Sea. *Neth J Aquat Ecol* 30(1):27–39
- De Lange HJ (2000) The attenuation of ultraviolet and visible radiation in Dutch inland waters. *Aquat Ecol* 34:215–226
- Dick S, Schönfeld W (1996) Transport and mixing in the North Frisian Wadden Sea- results of numerical investigations. *Deutsche Hydrographische Zeitschrift [German J Hydrogr]* 48(1):22
- Dijkema KS, Reijneck H-E, Wolff WJ (1980) Geomorphology of the Wadden Sea area. Report 1. Final report of the section 'Geomorphology' of the Wadden Sea Working Group, Leiden
- Doerffer R, Murphy D (1989) Factor analysis and classification of remotely sensed data for monitoring tidal flats. *Helgoländer Meeresun [Helgoland Mar Res]* 43:275–293
- Doerffer R, Schiller H (2006a) MERIS Case II ATBD-ATMO MERIS regional Case 2 Water BEAM extension atmospheric correction ATBD version 1.1, 24. November 2006, 25 pp
- Doerffer R, Schiller H (2006b) Algorithm theoretical basis document (ATBD) MERIS regional Case 2 water BEAM extension performance of the atmospheric correction part: sun glint correction MERIS Case 2 ATMO-Test, 14 p
- Doerffer R, Schiller H (2007) The MERIS Case 2 water algorithm. In *J Remote Sens* 28:517–535
- Doerffer R, Fischer J, Stössel M, Brockmann C, Grassl H (1989a) Analysis of thematic mapper data for studying the suspended matter distribution in the coastal area of the German bight (North Sea). *Remote Sens Environ* 28:61–73
- Doerffer R, Fischer J, Stössel M, Brockmann C, Grassl H (1989b) Small scale patches of suspended matter and phytoplankton in the Elbe River estuary, German Bight and tidal flats. *Adv Space Res* 9(1):191–200
- Doerffer R, Schiller H, Krasemann H, Heymann K, Cordes W, Schönfeld W, Röttgers R, Behner I, Kipp P (2003) MERIS Case 2 water validation early results North Sea/Helgoland/German Bight. In: *Proceedings of the ESA ENVISAT validation workshop 2002*, ESA Special publications SP-531
- Doxaran D, Froidefond J-M, Castaing P (2003) Remote-sensing reflectance of turbid sediment-dominated waters. Reduction of sediment type variations and changing illumination conditions effects by use of reflectance ratios. *Appl Optics* 42:2623–2634
- Doxaran D, Cherukuru RCN, Lavender SJ (2005) Use of reflectance band ratios to estimate suspended and dissolved matter concentrations in estuarine waters. In *J Remote Sens* 26:1763–1769
- Doxaran D, Cherukuru RCN, Lavender SJ (2006) Apparent and inherent optical properties of turbid estuarine waters: measurements, empirical quantification relationships, and modeling. *Appl Optics* 45:2310–2324
- Dupouy C, Arief D, Spitzer D (1983) Optical remote sensing of waters and tidal flats in western Wadden Sea. Internal Reports Royal Netherlands Institute for Sea Research (NIOZ) 2. NIOZ, Texel
- Eisma D, Kalf J (1996) In situ particle (floc) size measurement with the NIOZ in situ camera system. *J Sea Res* 36:49–53
- Eisma D, Bale AJ, Dearnaley MP, Fennessy MJ, Van Leussen W, Maldiney MA, Pfeiffer A, Wells JT (1996) Intercomparison of in situ suspended matter (floc) size measurements. *J Sea Res* 36:3–14
- ESA (2009) Technical information on satellite missions. <http://earth.esa.int/missions>. Accessed 5 June 2009
- EUMETSAT (2009) Technical information on the METEOSAT satellites. [www.eumetsat.int](http://www.eumetsat.int). Accessed 5 June 2009
- Flöser G (2004) Wadden Sea newsletter 2004, no 1. Common Wadden Sea secretariat (pp 8–10) Wilhelmshaven, Germany. ISSN 0922-7989
- Gade M, Alpers W, Melsheimer C, Tanck G (2008) Classification of sediments on exposed tidal flats in the German Bight using multi-frequency radar data. *Remote Sens Environ* 112:1603–1613
- Gallegos CL, Jordan TE, Hines AH, Weller DE (2005) Temporal variability of optical properties in a shallow, eutrophic estuary: seasonal and interannual variability. *Estuar Coast Shelf S* 64:156–170
- Gayer G, Dick S, Pleskachevsky A, Rosenthal W (2006) Numerical modeling of suspended matter transport in the North Sea. *Ocean Dynam* 56:62–77
- Gemein N, Stanev E, Brink-Spalink G, Wolff J-O, Reuter R (2006) Patterns of suspended matter in the East Frisian Wadden Sea: comparison of numerical simulations with MERIS observations. *EARSeL e-Proc* 5:180–198
- Gons HJ (1999) Optical teledetection of chlorophyll *a* in Turbid Inland waters. *Envi Sci Tech* 33:1127–1132
- Gons HJ, Rijkeboer M, Ruddick KG (2005) Effect of a waveband shift on chlorophyll retrieval from MERIS imagery of inland and coastal waters. *J Plankton Res* 27:125–127
- Gordon HR, Brown OB, Jacobs MM (1975) Computed relationships between the inherent and apparent optical properties of a flat homogeneous ocean. *Appl Optics* 14:417–427
- Grossart H-P, Brinkhoff T, Martens T, Duerselen C, Liebezeit G, Simon M (2004) Tidal dynamics of dissolved and particulate matter and bacteria in a tidal flat ecosystem in spring and fall. *Limnol Oceanogr* 49:2212–2222
- Hakvoort JHM, Heineke M, Heymann K, Kühl H, Riethmüller R, Witte G (1998) A basis for mapping the erodibility of tidal flats by optical remote sensing. *Mar Freshw Res* 49:867–873
- Hellweger FL, Schlosser P, Lall U, Weissel JK (2004) Use of satellite imagery for water quality studies in New York Harbor. *Estuar Coast Shelf S* 61:437–448
- Hoge FG, Swift RN (1982) Delineation of estuarine fronts in the German Bight using airborne laser-induced water Raman backscatter and fluorescence of water column constituents. *Int J Remote Sens* 3:475–495
- Højerslev NK (2002) On the small potential of color remote sensing of the sea waters between Norway, Sweden, Denmark, Germany and Poland. *Ocean Optics XVI*, Santa Fe CDROM, abstract 122



- Hommersom A, Peters S, Wernand MR, de Boer J (2009) Spatial and temporal variability in bio-optical properties of the Wadden Sea. *Estuar Coast Shelf S* 83:360–370
- Horstmann J, Koch W (2008) High resolution wind field retrieval from synthetic aperture radar: North Sea examples. In: Barale V, Gade M (eds) *Remote sensing of the European Seas*. Springer, The Netherlands, pp 331–342
- Houwing E-J (1999) Determination of the critical erosion threshold of cohesive sediments on intertidal mudflats along the Dutch Wadden Sea Coast. *Estuar Coast Shelf S* 49:545–555
- IOCCG (2000) Remote sensing of ocean colour in coastal, and other optically-complex, waters. Reports of the International Ocean-Colour Coordinating Group, No. 3, IOCCG, Dartmouth
- IOCCG (2009) Technical information on ocean colour satellite missions. [www.ioccg.org/sensors\\_ioccg.html](http://www.ioccg.org/sensors_ioccg.html). Accessed 5 June 2009
- Kerner M (2007) Effects of deepening the Elbe Estuary on sediment regime and water quality. *Estuar Coast Shelf S* 75:492–500
- Koponen S, Ruiz-Verdu A, Heege T, Heblinski J, Sorensen K, Kallio K, Pyhälähti T, Doerffer R, Brockmann C, Peters M (2008) Validation report. Development of MERIS lake water algorithms. Online, 65 pp
- Kromkamp JC, Morris EP, Forster RM, Honeywill C, Hagerthey S, Paterson DM (2006) Relationship of intertidal surface sediment chlorophyll concentration to hyperspectral reflectance and chlorophyll fluorescence. *Estuar Coasts* 29:183–196
- Laane RWPM (1980) Conservative behaviour of dissolved organic carbon in the Ems-Dollart estuary western Wadden Sea. *Neth J Sea Res* 14:192–199
- Laane RWPM (1982) Source of dissolved organic carbon in the Ems-Dollart estuary: the rivers and phytoplankton. *Neth J Sea Res* 15:331–339
- Laane RWPM, Koole L (1982) The relation between fluorescence and dissolved organic carbon in the Ems-Dollart estuary and the Western Wadden Sea. *Neth J Sea Res* 15:217–227
- Laane RWPM, Kramer KJM (1990) Natural fluorescence in the North Sea and its major estuaries. *Neth J Sea Res* 26:1–9
- Lanuru M, Riethmüller R, Van Bernem C, Heymann K (2007) The effect of bedforms (crest and trough systems) on sediment erodibility on a back-barrier tidal flat of the East Frisian Wadden Sea, Germany. *Estuar Coast Shelf S* 72:603–614
- Lehner S, Anders I, Gayer G (2004) High resolution maps of the suspended particulate matter concentration in the German Bight. *EARSeL e-Proc* 3(1/2004):118–126
- Lemke A, Lunau M, Stone J, Dellwig O, Simon M (2009) Spatio-temporal dynamics of suspended matter properties and bacterial communities in the back-barrier tidal flat system of Spiekeroog Island. *Ocean Dynam* 59:277–290
- Lettmann KA, Wolff JO, Badewien TH (2009) Modeling the impact of wind and waves on suspended particulate matter fluxes in the East Frisian Wadden Sea (southern North Sea). *Ocean Dynam* 59:239–262
- Lim HS, MatJafri MZ, Abdullah K, Alias AN, Rajab JM, Mohd Saleh N (2008) Algorithm for TSS Mapping using satellite data for Penang Island, Malaysia. In: Fifth international conference on computer graphics, imaging and visualisation 2008. CGIV, pp 376–379. doi:10.1109/CGIV.2008.18
- Lodhi MA, Rundquist DC, Han L, Kuzila MS (1997) The potential for remote sensing of loess soils suspended in surface waters. *J Am Water Res As* 33:111–117
- Lübben A, Dellwig O, Koch S, Beck M, Badewien TH, Fischer S, Reuter R (2009) Distributions and characteristics of dissolved organic matter in temperate coastal waters (Southern North Sea). *Ocean Dynam* 59:263–275
- Marees G, Wernand MR (1990) Optical data from the Dutch coastal waters, with reference to remote sensing applications. Internal reports Netherlands Institute for Sea Research (NIOZ) 1990–1991. NIOZ, Texel, the Netherlands 150 pp
- Michaelis H, Kolbe K, Thiessen A (1992) The “black spot disease” (anaerobic surface sediments) of the Wadden Sea. *Contr. ICES Statutory Meeting, Rostock, Code Nr. E.: 36, 11 S. ICES. C.M. E.: 36. 1–11. ICES Marine Environment Quality, Copenhagen. Denmark*
- Miller RL, McKee BA (2004) Using MODIS Terra 250 m imagery to map concentrations of total suspended matter in coastal waters. *Remote Sens Environ* 93(2004):259–266
- Mobley CD (1999) Estimation of the remote-sensing reflectance from above-surface measurements. *Appl Optics* 38:7442–7455
- NASA (2009) Technical information on satellite missions. <http://www.nasascience.nasa.gov/missions>. Accessed 5 June 2009
- Nechad B, De Cauwer V, Park Y, Ruddick K (2003) Suspended particulate matter (SPM) mapping from MERIS imagery. Calibration of a regional algorithm for the Belgian coastal waters, in MERIS user workshop, November 2003, Frascati. European Space Agency 200, 6 pp
- Niedermeier A, Hoja D, Lehner S (2005) Topography and morphodynamics in the German Bight using SAR and optical remote sensing data. *Ocean Dynam* 55:100–109
- Peperzak L (2002) The wax and wane of *Phaeocystis globosa* blooms. Dissertation, Groningen University
- Peters SWM, Vos RJ, Hoogenboom EJ, Hakvoort H, Van der Woerd H, Rijkeboer M, Pasterkamp R (2000) MERIMON-2000. MERIS for water quality monitoring in the Belgian-Dutch-German coastal zone. UPS-2 report 01–25. ISBN 90 54 11 370 7. The Netherlands Remote Sensing board. Rijkswaterstaat Survey Department, Delft
- Philippart CJM, Beukema JJ, Cadeé GC, Dekker R, Goedhart PW, Van Iperen JM, Leopold MF, Herman PMJ (2007) Impacts of nutrient reduction on coastal communities. *Ecosystems*. doi:10.1007/s10021-006-9006-7
- Pleskachevsky A, Gayer G, Horstmann J, Rosenthal W (2005) Synergy of satellite remote sensing and numerical modelling for monitoring of suspended particulate matter. *Ocean Dynam* 55:2–9
- Poremba K, Tillmann U, Hesse K-J (1999) Tidal impact on planktonic primary and bacterial production in the German Wadden Sea. *Helgoland Mar Res* 53:19–27
- Postma H (1954) Hydrography of the Dutch Wadden Sea. Dissertation, Groningen University
- Postma H (1960) Einige Bemerkungen über den Sinkstofftransport im Ems-Dollart Gebiet. [Some findings on the suspended matter transport in the Ems-Dollart area]. *Verhandelingen K.N.G.M.G. Deel XIX [Essays K.N.G.M.G. Part XIX]: 103–110*
- Postma H (1961) Transport and accumulation of suspended matter in the Dutch Wadden Sea. *Neth J Sea Res* 1:148–190
- Postma H (1982) Hydrography of the Wadden Sea: Movements and properties of water and particulate matter. Report 2. Final report of the section ‘Hydrography of the Wadden Sea Working Group. Leiden
- Puncken O, Badewien T, Reuter R (2006) MOSES (Measuring system for the observation of sea surfaces): Lagrangian drift experiments in the East Frisian Wadden Sea. In: Marcal A (ed) *EARSeL symposium proceedings, global developments in environmental earth observation from space*. Millpress, Rotterdam
- Rasmussen MB, Henriksen K, Jensen A (1983) Possible causes of temporal fluctuations in primary production of the microphytobenthos in the Danish Wadden Sea. *Mar Biol* 73:109–114
- Reise K, Herre E, Sturm M (1989) *Helgoländer Meeresun.* Helgoland Mar Res 43:417–433
- Reuter R, Diebel D, Hengstermann T (1993) Oceanographic laser remote sensing: measurement of hydrographic fronts in the German Bight and in the Northern Adriatic Sea. In *J Remote Sens* 14:823–848



- Reuter R, Badewien TH, Bartholomä A, Braun A, Lübken A, Rullkötter J (2009) A hydrographic time series station in the Wadden Sea (southern North Sea). *Ocean Dynam* 59:195–211
- Rijkswaterstaat (2008) Water Base. Database with in situ measurements. <http://www.waterbase.nl>. Accessed 19 June 2008
- Robinson IS, Antoine D, Darecki M, Gorringer P, Pettersson L, Rudick K, Santoleri R, Siegel HB, Vincent P, Wernand MR, Westbrook G, Zibordi G (2008) Remote sensing of shelf sea ecosystems: state of the art and perspectives. ESF marine board position paper, 12. European Science Foundation, ESF Marine Board, Strasbourg, 60 pp
- Roelse P (2002) Water en zand in balans. Evaluatie zandsuppleties na 1990; een morfologische beschouwing [Water and sand into balance. Evaluation zandsuppleties after 1990, a morphological consideration]. Rapport RIKZ/2002.003. Rijksinstituut voor Kust en Zee/RIKZ [State Institute for Coast and Sea/RIKZ]. LNO drukkerij uitgeverij, Zierikzee, the Netherlands. ISBN 90-36-369-3426-5. 108 pp
- Romeisner R (2007) Latest radar technology permits current measurements in coastal waters and rivers at sub-kilometer resolution. *Sea Technol* 48:44–46
- Romeisner R, Runge H (2008) Current measurements in European Coastal waters and rivers by along-track InSAR. In: Barale V, Gade M (eds) *Remote Sensing of the European Seas*. Springer, The Netherlands, pp 411–422
- Ruddick K, Park Y, Nechad B (2004) MERIS imagery of Belgian coastal waters: mapping of suspended particulate matter and chlorophyll-a. In: *Proceedings of the MERIS user workshop*, Frascati, Italy, 2003. ESA SP-549
- Santer R, Zagolski F (2009) ATBD—the MERIS level 1c. Issue 1, rev. 1, 6 Jan 2009, 15 pp
- Schiller K (2006) Derivation of photosynthetically available radiation from METEOSAT data in the German Bight with neural nets. *Ocean Dynam* 56:79–85
- Simis SGH (2006) Blue-green catastrophe: remote sensing of mass viral lysis of cyanobacteria. Dissertation, Vrije University Amsterdam. <http://hdl.handle.net/1871/10641>
- Spitzer D (ed) (1981) Balgzandproject 1981: optische remote-sensing van het water en het wadoppervlak: methoden en resultaten [Balgzandproject 1981: optic remote-sensing of the water and the mudflat surface: methods and results]. Internal Reports Royal Netherlands Institute for Sea Research (NIOZ) 7. NIOZ: Texel, The Netherlands. 130 pp
- Spitzer D, Folving S (1981) Remote optical measurements above the Danish Wadden area. Internal reports royal Netherlands institute for sea research (NIOZ) Netherlands 8. NIOZ. Texel, The Netherlands. 85 pp
- Spitzer D, Wernand MR (1981) In situ measurements of absorption spectra in the sea. *Deep-Sea Res* 28A:165–174
- SPOTimage (2009) Webpage with technical information on the SPOT satellites
- Stanev EV, Wolff J-O, Brink-Spalink G (2006) On the sensitivity of the sedimentary system in the East Frisian Wadden Sea to sea-level rise and wave-induced bed shear stress. *Ocean Dynam* 56:266–283
- Stanev EV, Brink-Spalink G, Wolff J-O (2007) Sediment dynamics in tidally dominated environments controlled by transport and turbulence: a case study for the East Frisian Wadden Sea. *J Geophys Res* 112:C04018. doi:10.1029/2005JC003045
- Stanev EV, Grayek S, Staneva J (2009) Temporal and spatial circulation patterns in the East Frisian Wadden Sea. *Ocean Dynam* 59:167–181
- Stelzer K, Brockmann C (2006) Optische Fernerkundung für die Küstenzone [Optical remote sensing for coastal zone]. In: Traub KP, Kohlus J (eds) *GIS im Küstenzonen Management. Grundlagen und Anwendungen [GIS in the coastal zone management. Fundamentals and Applications]* (pp 53–64) Wichmann Herbert. Heidelberg
- Tillmann U, Hesse K-J, Colijn F (2000) Planktonic primary production in the German Wadden Sea. *J Plankton Res* 22:1253–1276
- Van der Lee WTB (2000) The settling of mud flocs in the Dollard estuary, The Netherlands. Dissertation, Utrecht University
- Van Duin EHS, Blom G, Los FJ, Maffione R, Zimmerman R, Cerco CF, Dortch M, Best EPH (2001) Modeling underwater light climate in relation to sedimentation, resuspension, water quality and autotrophic growth. *Hydrobiologia* 444:25–42
- Van Ledden M (2003) Sand-mud segregation in estuaries and tidal basins. Dissertation, Technical University Delft
- Van Leussen W (1994) Estuarine macroflocs and their role in fine-grained sediment transport. Dissertation, University of Utrecht
- Van Leussen W, Van Velzen E (1989) High concentration suspensions: their origin and importance in Dutch estuaries and Coastal Waters. *J Coastal Res Special Issue no 5*:1–22
- Vinther N, Aagaard T, Nielsen J (2005) Complex sediment transport pattern on a spit-platform in the Danish Wadden Sea. *J Coastal Res* 21:710–719
- Visser MP (1970) The turbidity of the Southern North Sea. *Deutsche Hydrographische Zeitschrift [German Hydrographical Journal]* 23] 23:98–119
- Wang Y (1997) Satellite SAR imagery for topographic mapping of the tidal flat areas in the Dutch Wadden Sea. Dissertation, Vrije University Amsterdam
- Warnock RE, Gieskes WWC, Van Laar S (1999) Regional and seasonal differences in light absorption by yellow substance in the Southern Bight of the North Sea. *J Sea Res* 42:169–178
- Wernand MR, Spitzer D (1987) Processing of airborne CORSAIR data. Proceedings of the joint DFVLR/LAPAN- NIOZ workshop on remote sensing of the sea. Participation in the Snellius II expedition 1984. Reference Publication, TKH 8705. Indonesian National Institute of Aeronautics and Space (LAPAN), Jakarta, pp 153–159
- Wernand MR, Veldhuis MJW, Van der Woerd H-J (2006) Abstract 60020. Proceedings of the ocean optics OOXII conference, Montreal, Canada. CDROM, 156 MB
- Wimmer C, Siegmund R, Schwäbisch M, Moreira J (2000) Generation of high-precision DEMs of the Wadden Sea with airborne interferometric SAR. *IEEE T Geosci Remote* 38:25
- Winterwerp JC (1999) On the dynamics of high-concentrated mud suspensions. Dissertation, Technical University Delft
- Winterwerp JC, Van Kesteren WGM (2004) Introduction to the physics of cohesive sediment transport in the marine environment. Elsevier, the Netherlands. 576 pp
- Wolanski E, Chappell J, Ridd P, Vertessy R (1988) Fluidization of mud in estuaries. *J Geophys Res* 93:2351–2361
- Zhang Y, Liu M, Qin B, Van der Woerd HJ, Li J, Li Y (2009) Modeling remote-sensing reflectance and retrieving chlorophyll-a concentration in extremely turbid Case-2 waters (Lake Taihu, China) *IEEE T Geosci Remote* 47:1937–1948. doi:10.1109/TGRS.2008.2011892
- Zieler F (2008) Wave and current observations in European waters by ground-based X-band radar. In: Barale V, Gade M (eds) *Remote sensing of the European seas*. Springer, The Netherlands, pp 423–434
- Zimmerman JTF, Rommets JW (1974) Natural fluorescence as a tracer in the Dutch Wadden Sea and the adjacent North Sea. *Neth J Sea Res* 8:117–125